Solar Sailing

G. Gómez

IEEC & Dpt. de Matemàtiques i Informàtica, Universitat de Barcelona

3a Jornada de Sistemes Dinàmics a Catalunya
Institut d'Estudis Catalans
10 d'octubre de 2018

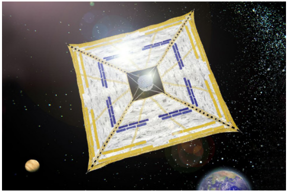

IKAROS – JAXA (2010–2015)
Interplanetary Kite-craft Accelerated by Radiation Of the Sun

Solar radiation pressure and solar sails

- Whereas **conventional rocket or spacecraft** is propelled by the thrust produced by its **internal engine** burn, a bright **mirror-like surface**, such as a solar sail, is pushed forward simply by **light from the Sun**.

- When a beam of light is pointed at a mirror-like surface, its photons reflect right back, just like a ball bouncing off a wall. In the process **the photons transmit their momentum** to the surface **twice** – once by the initial **impact**, and again by **reflecting back** from it.

Absorbed photons (F_a)

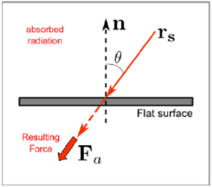

$$\mathbf{F}_a = P_{srp} A \langle \mathbf{n}, \mathbf{r}_s \rangle \mathbf{r}_s$$

Specular reflection (F_s)

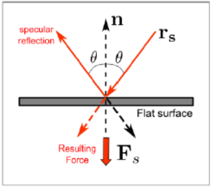

$$\mathbf{F}_s = 2 P_{srp} A \langle \mathbf{n}, \mathbf{r}_s \rangle^2 \mathbf{n}$$

- The **impact of sunlight photons** on the surface of a spacecraft or a sail produces **Solar Radiation Pressure (SRP)** acceleration.

Solar radiation pressure and solar sails

- In addition to the forces due to the absorbed photons and the specular reflection, there is also a **diffusive reflection** force.
- There is a whole range of “systems” that can produce **disturbances** in the orbit and attitude of a spacecraft **due to solar radiation pressure**. For example:
  - a sunshade
  - solar panels with flaps
  - reflective on-board structures
  - antennas
  - a generic reflective area
  - a solar sail
- From a dynamical point of view – it doesn't really matter which of these systems produces the SRP acceleration.
- A **solar sail** is made up of a reflective surface, or several surfaces, depending on the sail's design.
- From now on we will assume that the device is a solar sail.

Solar radiation pressure and solar sails

- Despite that SRP is small compared to other orbital perturbation, this extra acceleration becomes **relevant on long term propagations**.
- When the sail faces the Sun directly, it is subjected to a **flux of photons** that reflect off the surface and **impel the sail forward, away from the Sun.**
- By **changing the angle of the sail relative the Sun,** it is possible to **change the direction** in which the sail is propelled.
- Furthermore, **SRP manoeuvres** can also be obtained by **changing the reflectivity** of the sail (or by **changing the area to mass ratio**, such as folding part of a solar panel).
- A good modelling of SRP effect can help on:
  - **orbit determination** for GPS satellites,
  - **interplanetary mission** design,
  - **station keeping** at libration point orbits, like WFIRST.

Previous work and main references

- Mainly since 1999, after the work by **Colin R. McInnes**, extensive work has been done one the dynamics of solar sails, including SRP assisted maneuvers, in:
  - a two-body problem enviroment,
  - around the equilibrium points of the restricted three-body problem.
- The list of authors inludes: Hexi Baoyin, James D. Biggs, Ben Diedrich, Ariadna Farrés, Àngel Jorba, Marc Jorba, Jeannette Heiligers, Malcom Macdonald, Colin R. McInnes, Allan I. S. McInnes, Giorgio Mingotti, Jules Simo, Patricia Verrier, Thomas J. Waters, etc.
- Three important references are:
  - **Colin R. McInnes**. *Solar sailing: technology, dynamics and mission applications*. Springer-Verlag, 1999.
  - **Ariadna Farrés**. *Contribution to the Dynamics of a Solar Sail in the Earth-Sun System*. Phd thesis, Universitat de Barcelona, 2009.
  - **Malcom Macdonald**, editor. *Advances in Solar Sailing*. Springer Praxis, 2014.

This talk

Most of the contents of this talk can be found in:

- Colin R. McInnes. *Solar sailing: technology, dynamics and mission applications*. Springer-Verlag, 1999.
- Setefania Soldini, Josep J. Masdemont, Gerard Gómez. *Dynamics of Solar Radiation Pressure assisted Manoeuvres between Lissajous Orbits*. To appear in Journal of Guidance, Control, & Dynamics.
- Xun Duan, Gerard Gómez, Josep J. Masdemont, Yue Xiaokui. *Solar Sail Propellant–Free Transfer Maneuvers Between Libration Point Orbits Around the Collinear Equilibrium Points*. 69th International Astronautical Congress, Bremen 2018, Paper No. IAC-18-C1,2,1.
- And, of course, Wikipedia.

Are there many missions using solar sails?

- The world's first interplanetary solar sail spacecraft was **IKAROS**, that was launched in 2010, along with **Akatsuki**, by the Japanese space agency JAXA.

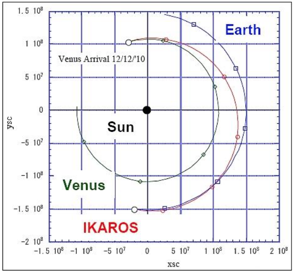

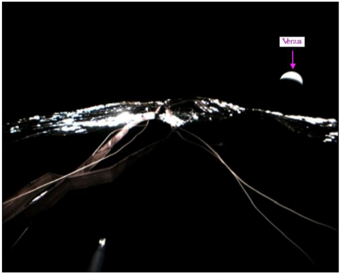

- On December 2010, IKAROS passed by Venus at about 80,800 km.
- IKAROS was a 200 m^2 solar sail, and the total SRP effect over the six month flight was of 100 m/s.
- IKAROS had a few science instruments aboard - a gamma ray detector and a dust particle counter, and also small solar panels embedded in the sail, which provided power to the satellite.
- IKAROS surpassed its initial mission timeline, which was 6 months, and continued to communicate with Earth until 2015.

Other missions using SRP

- Both the **Mariner 10** mission (NASA, 1973–1975), which flew by the planets Mercury and Venus, and the **MESSENGER** mission to Mercury (NASA, 2011–2015), demonstrated the use of SRP as a method of **attitude control** in order to conserve attitude-control propellant.

- **Hayabusa** (JAXA, 2003–2005) also used SRP as a method of **attitude control** to compensate for broken reaction wheels and chemical thruster.

  Hayabusa was robotic spacecraft developed to return a sample of material from a small near-Earth asteroid named 25143 Itokawa to Earth.

- In June 21, 2005, a joint private project between Planetary Society, Cosmos Studios and Russian Academy of Science launched a prototype sail **Cosmos 1** from a submarine in the Barents Sea, but the Volna rocket failed and the spacecraft could not reach its orbit.

- The NASA **NanoSail-D** was lost in a launch failure aboard a Falcon 1 rocket on August 3, 2008.

- The NASA **NanoSail-D2**, which was launched on a Minotaur IV on November 19, 2010, becoming NASA's first solar sail deployed in low earth orbit.

The Solar Radiation Pressure acceleration

The SRP model, that will be used in what follows, only considers the specular reflection force.

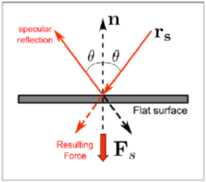

The SRP acceleration is then:

$$\mathbf{a}^{srp} = \beta \frac{1-\mu}{r^2} \langle \hat{\mathbf{r}}, \mathbf{n} \rangle^2 \mathbf{n}$$

where:

- $\beta \in (0,1)$ is the lightness parameter, related to the spacecraft's reflectivity, and the area-to-mass ratio,
- $\mathbf{n}$ is the unitary normal vector to the surface of the sail ($\mathbf{n}$ depends on two angles α and δ),
- α is the cone angle,
- δ is the clock angle,
- $\hat{\mathbf{r}} = \mathbf{r}/r$ is in the unitary vector in the Sun-sail direction,
- r is the distance from the Sun to the sail.

The sail orientation angles α and δ

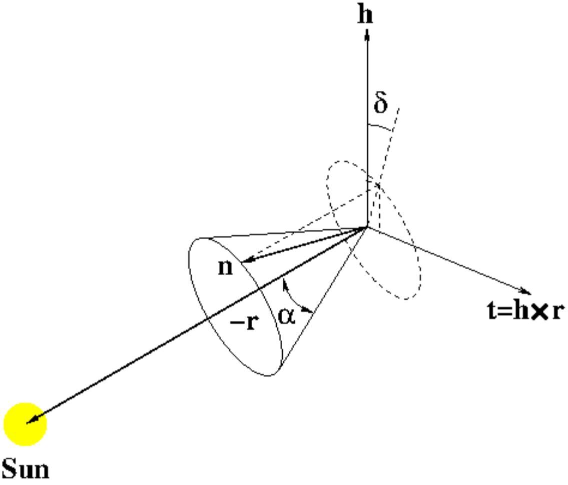

Schematic representation of the cone angle α and the clock angle δ

Non-Keplerian 2-body orbits

- Consider the classical 2-body problem (Sun–sail) with an additional SRP acceleration acting on the solar sail.
- The dynamics will be formulated in a rotating frame of reference (x, y, z).
- The fixed points of the resulting equations will be non-Keplerian 2-body orbits (displaced orbits) when viewed from an inertial frame of reference $(X, Y, Z = z)$.

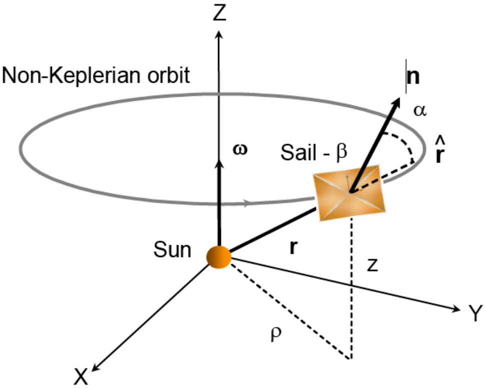

Displaced non-Keplerian 2-body orbits

- Consider a spacecraft (sail) of mass m at position $\boldsymbol{r}$ in a rotating frame of reference (x, y, z) that rotates with **constant** angular velocity $\boldsymbol{\omega}$ relative to an inertial frame (X, Y, Z).

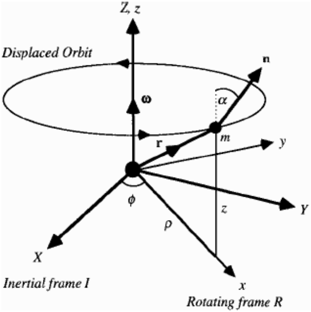

- The equation of motion of the sail in the rotating frame is

$$\ddot{\boldsymbol{r}} + 2\boldsymbol{\omega} \times \dot{\boldsymbol{r}} + \boldsymbol{\omega} \times (\boldsymbol{\omega} \times \boldsymbol{r}) = \boldsymbol{a}^{srp} - \nabla\Omega$$

where Ω is the gravitational potential of the central body, and $\mathbf{a}^{srp}$ the solar radiation pressure acceleration:

$$\Omega = -\frac{\mu}{r}, \qquad \mathbf{a}^{srp} = \beta \frac{1-\mu}{r^2} \langle \hat{\mathbf{r}}, \mathbf{n} \rangle^2 \mathbf{n}.$$

Displaced non-Keplerian 2-body orbits

- The above equation of motion

$$\ddot{\boldsymbol{r}} + 2\boldsymbol{\omega} \times \dot{\boldsymbol{r}} + \boldsymbol{\omega} \times (\boldsymbol{\omega} \times \boldsymbol{r}) = \boldsymbol{a}^{srp} - \nabla \Omega$$

  may be simplified by introducing a new potential V to represent the centripetal acceleration

$$\nabla V = \boldsymbol{\omega} \times (\boldsymbol{\omega} \times \boldsymbol{r}), \quad V = -\frac{1}{2} \|\boldsymbol{\omega} \times \boldsymbol{r}\|.$$

- Defining a new augmented potential function

$$U = \Omega + V$$

  the equation of motion becomes

$$\ddot{\boldsymbol{r}} + 2\boldsymbol{\omega} \times \dot{\boldsymbol{r}} + \nabla U = \boldsymbol{a}^{srp}.$$

Displaced non-Keplerian 2-body orbits

- The conditions for equilibrium solutions are obtained by setting $\ddot{\boldsymbol{r}} = \dot{\boldsymbol{r}} = 0$, so

$$\ddot{\boldsymbol{r}} + 2\boldsymbol{\omega} \times \dot{\boldsymbol{r}} + \nabla U = \boldsymbol{a}^{srp} \quad \Rightarrow \quad \nabla U = \boldsymbol{a}^{srp}.$$

- Taking now the cross product with $\boldsymbol{n}$, it is found that

$$\nabla U \times \boldsymbol{n} = 0 \quad \Rightarrow \quad \boldsymbol{n} = \lambda \, \nabla U$$

  where λ is an arbitrary scalar.

- Since $\|\boldsymbol{n}\| = 1$

$$\lambda = \|\nabla U(\boldsymbol{r})\|^{-1}$$

  so, the required SRP thrust vector orientation for an equilibrium solution in the rotating frame is given by

$$\boldsymbol{n} = \frac{\nabla U}{\|\nabla U(\boldsymbol{r})\|}.$$

Displaced non-Keplerian 2-body orbits

- Because $\boldsymbol{\omega}$ is constant, there can be no transverse component of thrust, so that the SRP thrust vector is in the plane spaned by the radius vector $\boldsymbol{r}$ and the vertical axis $\boldsymbol{z}$.

  Therefore, the thrust vector orientation may be defined by a single angle α.

- The determination of α is done taking vector and scalar products of $\boldsymbol{n} = \frac{\nabla U}{\|\nabla U(\boldsymbol{r})\|}$ with $\hat{\mathbf{r}}$, so:

$$\tan\alpha = \frac{\|\hat{\boldsymbol{r}} \times \nabla U\|}{\langle \hat{\boldsymbol{r}}, \nabla U \rangle}.$$

- Similarly, the required solar sail lightness number β is obtained taking a scalar product of the equation of motion

$$\ddot{\boldsymbol{r}} + 2\boldsymbol{\omega} \times \dot{\boldsymbol{r}} + \nabla U = \boldsymbol{a}^{srp}$$

  with $\boldsymbol{n}$, and requiring the equilibrium conditions

$$\beta = \frac{r^2 \langle \nabla U, \boldsymbol{n} \rangle}{\mu \langle \hat{\mathbf{r}}, \mathbf{n} \rangle^2}.$$

Displaced non-Keplerian 2-body orbits

- Using cylindrical coordinates (ρ, ϕ, z), the rotating two-body potential function can be written as

$$U = -\left(\frac{1}{2}\rho^2\omega^2 + \frac{\mu}{r}\right)$$

where the angular velocity ω is related to the orbit period T by $\omega = 2\pi/T$.

- Evaluating the potential gradient, and substituting in the above equations for α and β, we get

$$\tan\alpha = \frac{(z/\rho)(\omega/\tilde{\omega})^2}{(z/\rho)^2 + [1 - (\omega/\tilde{\omega})^2]},$$

$$\beta = \left[1 + \left(\frac{z}{\rho}\right)^2\right]^{1/2} \frac{\left((z/\rho)^2 + [1 - (\omega/\tilde{\omega})^2]^2\right)^{3/2}}{\left((z/\rho)^2 + [1 - (\omega/\tilde{\omega})^2]\right)^2}$$

where $\tilde{\omega}$ is the orbital angular velocity of a circular Keplerian orbit of radius r.

Displaced 1-year non-Keplerian 2-body orbits

- The above equations depend only on z/ρ and $\omega/\tilde{\omega}$, so that they have a scale invariance.
- In addition, the expressions are also independent of the azimuthal angle ϕ. Therefore, for a fixed solar sail lightness number the second equation defines nested surfaces of revolution about the z-axis.

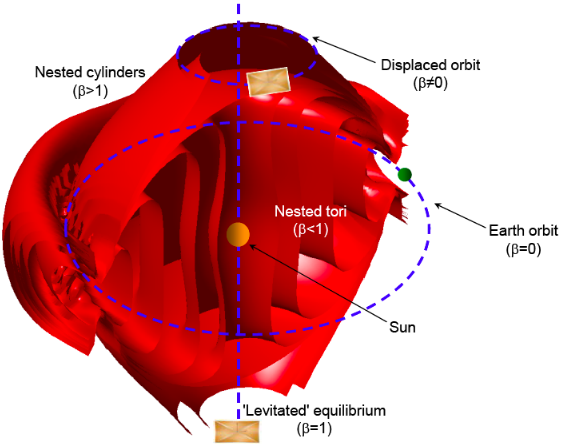

Lissajous orbits around the equilibrium points of the CR3BP

The equations of motion of the model, in the usual rotating reference frame, are

$$\begin{cases} \ddot{X} - 2\dot{Y} &= \Omega_X + a_X^{srp} \\ \ddot{Y} + 2\dot{X} &= \Omega_Y + a_Y^{srp} \\ \ddot{Z} &= \Omega_Z + a_Z^{srp} \end{cases}$$

where

- $\Omega(X, Y, Z)$ is the usual CR3BP effective potential

$$\Omega(X, Y, Z) = \frac{1}{2}(X^2 + Y^2) + \frac{1-\mu}{r_1} + \frac{\mu}{r_2} + \frac{1}{2}\mu(1-\mu)$$

- r_1 and r_2 are, respectively, the distances from the solar sail to the Sun and the Earth

$$\begin{aligned} r_1^2 &= (X-\mu)^2 + Y^2 + Z^2 \\ r_2^2 &= (X-\mu+1)^2 + Y^2 + Z^2 \end{aligned}$$

- a_X^{srp},a_Y^{srp},a_Z^{srp} are the three components of the SRP acceleration $\boldsymbol{a}^{srp}$.

The solar radiation pressure acceleration

Using the three solar sail parameters α, δ and β, the components of the SRP acceleration $\mathbf{a}^{srp}$ can be written as

$$
\begin{aligned}
a_X^{srp} &= \frac{\beta(1-\mu)(X-\mu)}{|\boldsymbol{r}|^3}\cos^3\alpha - \frac{\beta(1-\mu)(X-\mu)Z}{|\boldsymbol{r}|^2|(\boldsymbol{r}\times\hat{\boldsymbol{z}})\times\boldsymbol{r}|}\cos^2\alpha\sin\alpha\cos\delta \\
&\quad + \frac{\beta(1-\mu)Y}{|\boldsymbol{r}|^2|(\boldsymbol{r}\times\hat{\boldsymbol{z}})|}\cos^2\alpha\sin\alpha\sin\delta, \\
a_Y^{srp} &= \frac{\beta(1-\mu)Y}{|\boldsymbol{r}|^3}\cos^3\alpha - \frac{\beta(1-\mu)YZ}{|\boldsymbol{r}|^2|(\boldsymbol{r}\times\hat{\boldsymbol{z}})\times\boldsymbol{r}|}\cos^2\alpha\sin\alpha\cos\delta \\
&\quad - \frac{\beta(1-\mu)(X-\mu)}{|\boldsymbol{r}|^2|(\boldsymbol{r}\times\hat{\boldsymbol{z}})|}\cos^2\alpha\sin\alpha\sin\delta, \\
a_Z^{srp} &= \frac{\beta(1-\mu)Z}{|\boldsymbol{r}|^3}\cos^3\alpha - \frac{\beta(1-\mu)(Y^2+(X-\mu)^2)}{|\boldsymbol{r}|^2|(\boldsymbol{r}\times\hat{\boldsymbol{z}})\times\boldsymbol{r}|}\cos^2\alpha\sin\alpha\cos\delta.
\end{aligned}
$$

Equilibrium points of the equations of motion

- The equilibrium points of the equations of motion satisfy

  $$\nabla\Omega + \mathbf{a}^{srp} = 0$$

  and since

  $$\mathbf{a}^{srp} = \beta \frac{1-\mu}{r^2} \langle \hat{\mathbf{r}}, \mathbf{n} \rangle^2 \mathbf{n}$$

  $\mathbf{n}$ has to be aligned with $\nabla\Omega$ (as in the 2-body case).

- These "artificial equilibrium points" have been studied by many authors, including
  - C. R. McInnes, *Solar sailing: technology, dynamics and mission applications*. Springer, 1998.
  - Ariadna Farrés, *Contribution to the dynamics of a solar sail in the Earth-Sun system*. PhD UB, 2009.

Equilibrium points of the equations of motion for $\delta = \pi/2$

- When the clock angle δ is equal to $\pi/2$, the artificial equilibrium points are on the $X - Y$ plane, and their coordinates (γ_1, γ_2) are the solution of the system

$$
\begin{aligned}
\gamma_1 - & \frac{\mu(\gamma_1 - \mu + 1)}{((\gamma_1 - \mu + 1)^2 + \gamma_2^2)\sqrt{(\gamma_1 - \mu + 1)^2 + \gamma_2^2}} + \\
& + \frac{(1-\mu)\left[-\gamma_1 + \mu + \beta \cos^2 \alpha \left[(\gamma_1 - \mu)\cos\alpha + \gamma_2 \sin\alpha\right]\right]}{((\gamma_1 - \mu)^2 + \gamma_2^2)\sqrt{(\gamma_1 - \mu)^2 + \gamma_2^2}} = 0, \\
\gamma_2 - & \frac{\mu\gamma_2}{((\gamma_1 - \mu + 1)^2 + \gamma_2^2)\sqrt{(\gamma_1 - \mu + 1)^2 + \gamma_2^2}} + \\
& + \frac{(1-\mu)\left[-\gamma_2 + \beta \cos^2 \alpha \left[\gamma_2 \cos\alpha - (\gamma_1 - \mu)\sin\alpha\right]\right]}{((\gamma_1 - \mu)^2 + \gamma_2^2)\sqrt{(\gamma_1 - \mu)^2 + \gamma_2^2}} = 0.
\end{aligned}
$$

Location of the planar libration points SL_2 and SL_1 for $\delta = \pi/2$

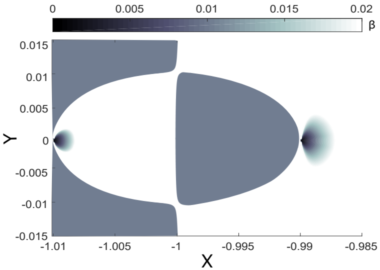

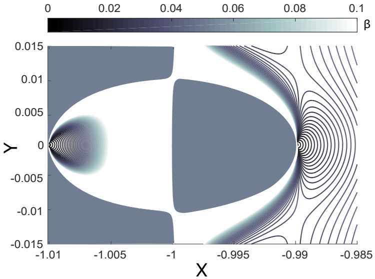

$\beta = 0$ up to 0.02 $\qquad$ $\beta = 0$ up to 0.1

Position of the planar libration points SL_2 ($X \approx -1.01$) and SL_1 ($X \approx -0.99$) in the vicinity of the Earth ($X \approx -1.0$

- The shaded regions are non-feasible locations due to the constraint $\cos\alpha = \boldsymbol{r}^T \boldsymbol{n} \geq 0$
- Each colored scale line gives the position of the libration points for $\alpha \in (-\pi/2, \pi/2)$ when the lightness parameter β is fixed
- When $\alpha = \pm\pi/2$, all the curves collapse to the position of the equilibrium points of the CR3BP, since no SRP force is applied

The equilibrium points SL_i

- If $\alpha = \pm\pi/2$, then $\mathbf{n} \perp \mathbf{r}$, so $\boldsymbol{a}^{srp} = 0$. In this case the equations of motion coincide with the ones of the CR3BP, and $SL_i = L_i$ for $i = 1, ..., 5$.
- If $\alpha = 0$ (Sun-pointing sail), the force due to the SRP is aligned with the gravitational attraction of the Sun, so the model can be seen as the usual CR3BP with the mass of the Sun $1 - \mu$ decreased
- If $\alpha = 0$, the SL_1 and SL_2 points are located on the X axis, and move towards the Sun as the value of β increases
- If $\alpha = 0$, the position of SL_1 and SL_2 can be determined by means of an equation similar to Euler's quintic equation for the CR3BP

Stability of SL_1 for $\alpha \in [-\pi/2, \pi/2]$, $\delta = \pi/2$

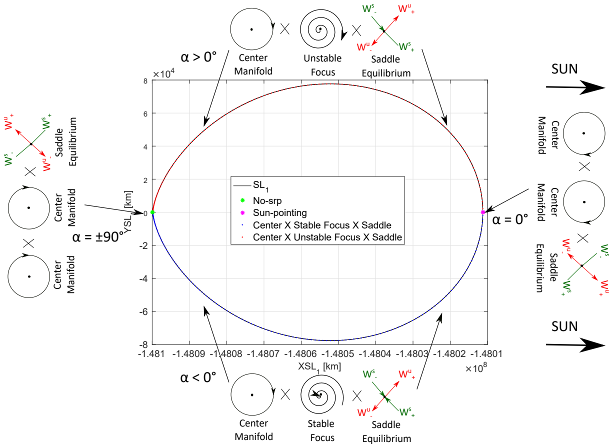

- When $\alpha = 0, \pm\pi/2$, then: $Y_{SL1} = 0$, $\lambda_{1,2} = \pm\lambda \in \mathbb{R}$, $\lambda_{3,4} = \pm\omega i$ and $\lambda_{5,6} = \pm\nu i$ (center $\times$ center $\times$ saddle)
- When $\alpha < 0$, then $Y_{SL1} < 0$, $\lambda_{1,2} \approx \pm\lambda \in \mathbb{R}$, $\lambda_{3,4} = \eta \pm \omega i$ ($\eta > 0$ small), and $\lambda_{5,6} = \pm\nu i$ (center $\times$ stable focus $\times$ saddle)
- When $\alpha > 0$, then $Y_{SL1} > 0$, $\lambda_{1,2} \approx \pm\lambda \in \mathbb{R}$, $\lambda_{3,4} = \eta \pm \omega i$ ($\eta < 0$ small), and $\lambda_{5,6} = \pm\nu i$ (center $\times$ unstable focus $\times$ saddle)

The important fact!

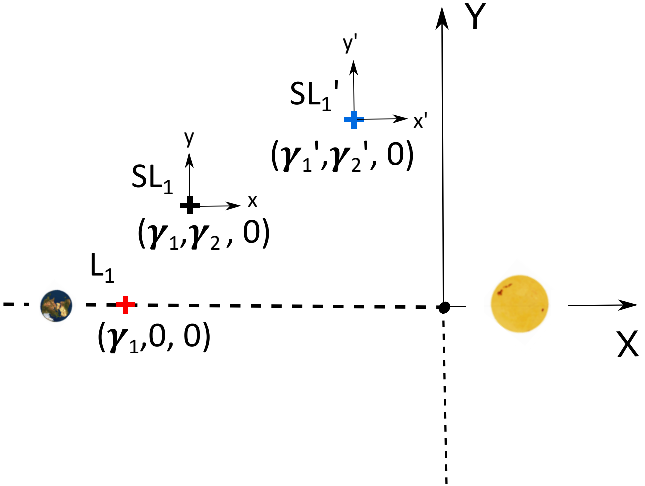

The position of the equilibrium points changes with the sail parameters, this allows to perform transfers between libration point orbits without Δv. The same is true in the 3D case.

The $SL_1(\alpha, \delta)$ families of equilibrium points for $\alpha \in [-\pi/2,\ \pi/2]$, $\delta \in (0, 2\pi)$, and several values of β

- For small values of β, $SL_1(\alpha, \delta)$ is a sphere, when $\beta \in (0.03, 0.07)$ then $SL_1(\alpha, \delta)$ has two components, and for $\beta > 0.07$ one of the two components (the one in blue in the plots) merges with the SL families associated to L_3, L_4 and L_5.

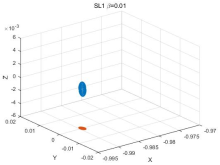

$\beta = 0.01$

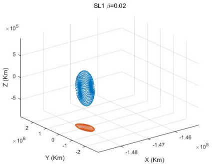

$\beta = 0.02$

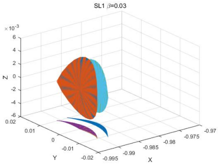

$\beta = 0.03$

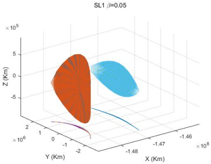

$\beta = 0.05$

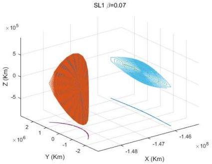

$\beta = 0.07$

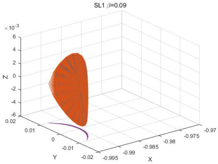

$\beta = 0.09$

The $SL_2(\alpha, \delta)$ families of equilibrium points for $\alpha \in [-\pi/2, \ \pi/2]$ and $\delta \in (0, 2\pi)$, and several values of β

- When $\alpha \in [-\pi/2, \ \pi/2]$, $\delta \in (0, 2\pi)$, and β is fixed, the equilibrium points $SL_2(\alpha, \delta)$ define a 2D surface homeomorphic to a sphere; each equilibrium point on the sphere corresponds to a given sail orientation.

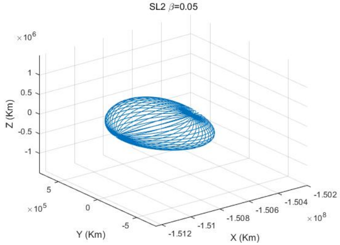

$\beta = 0.05$

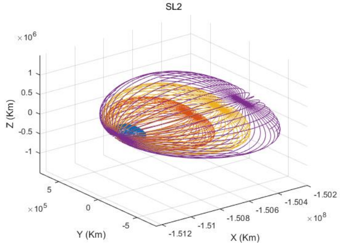

$\beta = 0.01, \ 0.05, \ 0.09, \ 0.13$

Behaviour of the central manifold of the L_1 point in the CR3BP+SRP

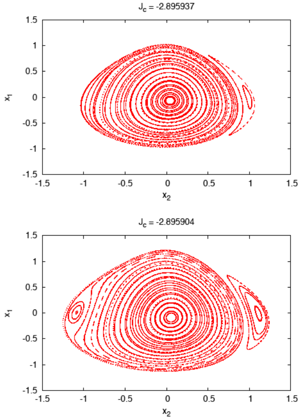

Poincaré map representation of the flow around the L_1 point for $\tilde{\alpha} = 0$, $\tilde{\delta} = 0.01$. (A. Farrés, "Contribution to the Dynamics of a Solar Sail in the Earth - Sun System," PhD Thesis, 2009.)

The linear equations of motion around the equilibrium points SL_1 and SL_2

The linear equations of motion around the equilibrium points are:

$$\left\{ \begin{array}{rcl} \ddot{x} - 2\dot{y} & = & a_1 x + a_2 y + a_3 z \\ \ddot{y} + 2\dot{x} & = & b_1 x + b_2 y + b_3 z \\ \ddot{z} & = & c_1 x + c_2 y + c_3 z \end{array} \right.$$

where the a_i, b_i and c_i depend on μ and the sail parameters

$$a_0 = -A_1 \mp \frac{\mu}{\gamma} + \frac{1-\mu}{\gamma^3}\frac{A_1}{D_1^3} + \frac{\mu}{\gamma^3}\frac{A_2}{D_2^3} - \frac{\beta(1-\mu)\cos^2\alpha}{\gamma^3 D_1^3 D_3}(A_1 D_3 \cos\alpha + C_1 A_1 \sin\alpha\cos\delta + B_1 D_1 \sin\alpha\sin\delta),$$

$$a_1 = 1 + \frac{1-\mu}{\gamma^3}\frac{3A_1^2 - D_1^2}{D_1^5} + \frac{\mu}{\gamma^3}\frac{3A_2^2 - D_2^2}{D_2^5} - \frac{\beta(1-\mu)\cos^2\alpha}{\gamma^3 D_1^3 D_3}\left(\frac{(3A_1^2 - D_1^2)D_3}{D_1^2}\cos\alpha + C_1(E_3 A_1^2 - 1)\sin\alpha\cos\delta + B_1 E_2 A_1 D_1 \sin\alpha\sin\delta\right),$$

$$a_2 = \frac{1-\mu}{\gamma^3}\frac{3A_1 B_1}{D_1^5} + \frac{\mu}{\gamma^3}\frac{3A_2 B_2}{D_2^5} - \frac{\beta(1-\mu)\cos^2\alpha}{\gamma^3 D_1^3 D_3}\left(\frac{3A_1 B_1 D_3}{D_1^2}\cos\alpha + E_3 B_1 A_1 C_1 \sin\alpha\cos\delta + (E_2 B_1^2 - 1)D_1 \sin\alpha\sin\delta\right),$$

$$a_3 = \frac{1-\mu}{\gamma^3}\frac{3A_1 C_1}{D_1^5} + \frac{\mu}{\gamma^3}\frac{3A_2 C_2}{D_2^5} - \frac{\beta(1-\mu)\cos^2\alpha}{\gamma^3 D_1^3 D_3}\left(\frac{3A_1 C_1 D_3}{D_1^2}\cos\alpha + A_1\left(\frac{3C_1^2}{D_1^2} - 1\right)\sin\alpha\cos\delta + \frac{2B_1 C_1}{D_1}\sin\alpha\sin\delta\right),$$

$$b_0 = -B_1 + \frac{1-\mu}{\gamma^3}\frac{B_1}{D_1^3} + \frac{\mu}{\gamma^3}\frac{B_2}{D_2^3} - \frac{\beta(1-\mu)\cos^2\alpha}{\gamma^3 D_1^3 D_3}(B_1 D_3 \cos\alpha + C_1 B_1 \sin\alpha\cos\delta - A_1 D_1 \sin\alpha\sin\delta),$$

$$b_1 = \frac{1-\mu}{\gamma^3}\frac{3A_1 B_1}{D_1^5} + \frac{\mu}{\gamma^3}\frac{3A_2 B_2}{D_2^5} - \frac{\beta(1-\mu)\cos^2\alpha}{\gamma^3 D_1^3 D_3}\left(\frac{3A_1 B_1 D_3}{D_1^2}\cos\alpha + E_3 B_1 A_1 C_1 \sin\alpha\cos\delta - (E_2 A_1^2 - 1)D_1 \sin\alpha\sin\delta\right),$$

$$b_2 = 1 + \frac{1-\mu}{\gamma^3}\frac{3B_1^2 - D_1^2}{D_1^5} + \frac{\mu}{\gamma^3}\frac{3B_2^2 - D_2^2}{D_2^5} - \frac{\beta(1-\mu)\cos^2\alpha}{\gamma^3 D_1^3 D_3}\left(\frac{(3B_1^2 - D_1^2)D_3}{D_1^2}\cos\alpha + C_1(E_3 B_1^2 - 1)\sin\alpha\cos\delta - B_1 E_2 A_1 D_1 \sin\alpha\sin\delta\right),$$

$$b_3 = \frac{1-\mu}{\gamma^3}\frac{3B_1 C_1}{D_1^5} + \frac{\mu}{\gamma^3}\frac{3B_2 C_2}{D_2^5} - \frac{\beta(1-\mu)\cos^2\alpha}{\gamma^3 D_1^3 D_3}\left(\frac{3B_1 C_1 D_3}{D_1^2}\cos\alpha + B_1\left(\frac{3C_1^2}{D_1^2} - 1\right)\sin\alpha\cos\delta - \frac{2A_1 C_1}{D_1}\sin\alpha\sin\delta\right),$$

....

The solution of the linear equations

- The solution of the above linear equations can be written as:

$$
\begin{aligned}
x(t) &= A_1 e^{\lambda_1 t} + A_2 e^{\lambda_2 t} \\
&+ A_3 e^{\eta_1 t} \cos\omega_1 t + A_4 e^{\eta_1 t} \sin\omega_1 t \\
&+ A_5 e^{\eta_2 t}(\overline{k}_5 \cos\omega_2 t + \overline{k}_6 \sin\omega_2 t) + A_6 e^{\eta_2 t}(\overline{k}_5 \sin\omega_2 t - \overline{k}_6 \cos\omega_2 t) \\
y(t) &= A_1 k_1 e^{\lambda_1 t} + A_2 k_2 e^{\lambda_2 t} \\
&+ A_3 e^{\eta_1 t}(k_3 \cos\omega_1 t + k_4 \sin\omega_1 t) + A_4 e^{\eta_1 t}(k_3 \sin\omega_1 t - k_4 \cos\omega_1 t) \\
&+ A_5 e^{\eta_2 t}(k_5 \cos\omega_2 t + k_6 \sin\omega_2 t) + A_6 e^{\eta_2 t}(k_5 \sin\omega_2 t - k_6 \cos\omega_2 t) \\
z(t) &= A_1 \overline{k}_1 e^{\lambda_1 t} + A_2 \overline{k}_2 e^{\lambda_2 t} \\
&+ A_3 e^{\eta_1 t}(\overline{k}_3 \cos\omega_1 t + \overline{k}_4 \sin\omega_1 t) + A_4 e^{\eta_1 t}(\overline{k}_3 \sin\omega_1 t - \overline{k}_4 \cos\omega_1 t) \\
&+ A_5 e^{\eta_2 t} \cos\omega_2 t + A_6 e^{\eta_2 t} \sin\omega_2 t
\end{aligned}
$$

  where $A_1, ..., A_6$ are arbitrary parameters, the values of k_i and $\overline{k}_i$, depend on the coefficients of the linear differential equations, and the λ_i are the roots of the characteristic polynomial

- This solution can be also written in matrix form as

$$[x(t),\, y(t),\, z(t),\, \dot{x}(t),\, \dot{y}(t),\, \dot{z}(t)]^T = H(t)\,[A_1,\, A_2,\, A_3,\, A_4,\, A_5,\, A_6]^T$$

  Inverting this system for $t = 0$ we get the values of the coefficients A_i as a function of the initial conditions

The solution of the linear equations

- It is also convenient to write the above oscillatory solutions using amplitudes and phases
- We define
  - the unstable and stable amplitudes

$$A_u = A_1, \quad A_s = A_2$$

  - the planar (in-plane) and vertical (out-off-plane) amplitudes

$$A_x = \sqrt{A_3^2 + A_4^2}, \quad A_z = \sqrt{A_5^2 + A_6^2}$$

  - the phases ϕ_1 and ϕ_2

$$A_3 = A_x \cos\phi_1, \quad A_4 = -A_x \sin\phi_1, \quad A_5 = A_z \cos\phi_2, \quad A_6 = -A_z \sin\phi_2$$

The solution of the linear equations

Using the new amplitudes and phases, the solution of the linear equations becomes

$$x(t) = A_u e^{\lambda_1 t} + A_s e^{\lambda_2 t} + A_x e^{\eta_1 t}\cos(\omega_1 t + \phi_1) + A_z e^{\eta_2 t}\overline{k}_{56}\cos(\omega_2 t + \overline{\phi}_{56})$$
$$y(t) = A_u k_1 e^{\lambda_1 t} + A_s k_2 e^{\lambda_2 t} + A_x e^{\eta_1 t} k_{34}\cos(\omega_1 t + \phi_{34}) + A_z e^{\eta_2 t} k_{56}\cos(\omega_2 t + \phi_{56})$$
$$z(t) = A_u \overline{k}_1 e^{\lambda_1 t} + A_s \overline{k}_2 e^{\lambda_2 t} + A_x e^{\eta_1 t}\overline{k}_{34}\cos(\omega_1 t + \overline{\phi}_{34}) + A_z e^{\eta_2 t}\cos(\omega_2 t + \phi_2)$$

where $\lambda_1 > 0$, $\lambda_2 < 0$, $\lambda_{3,4} = \eta_1 \pm i\omega_1$, and $\lambda_{5,6} = \eta_2 \pm i\omega_2$ are the roots of:

$$\begin{aligned}
\lambda^6 - (a_1 + b_2 + c_3 - 4)\lambda^4 + (2a_2 - 2b_1)\lambda^3 \\
-(4c_3 - a_1 b_2 + a_2 b_1 - a_1 c_3 + a_3 c_1 - b_2 c_3 + b_3 c_2)\lambda^2 \\
-2(a_2 c_3 - a_3 c_2 - b_1 c_3 + b_3 c_1)\lambda \\
-a_3 b_1 c_2 - a_2 b_3 c_1 - a_1 b_2 c_3 + a_3 b_2 c_1 + a_2 b_1 c_3 + a_1 b_3 c_2 = \; 0
\end{aligned}$$

- A_u and A_s are the unstable and stable amplitudes of the solution
- A_x and A_z are the planar (in-plane) and vertical (out-off-plane) amplitudes of the solution
- ϕ_1 and ϕ_2 are the phases that determine the initial condition for $t = t_0$. The remaining angles ϕ_{34}, ϕ_{56}... are functions of ϕ_1 and ϕ_2

Examples of solutions of the linear equations

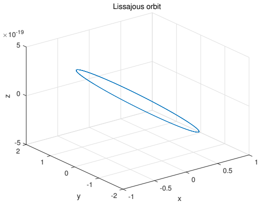

Planar oscillation

$A_u = 0,\ A_s = 0,\ A_x = 0.771,\ A_z = 0$

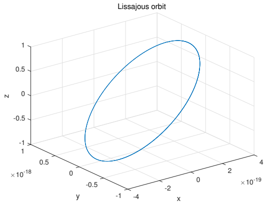

Vertical oscillation

$A_u = 0,\ A_s = 0,\ A_x = 0,\ A_z = 0.906$

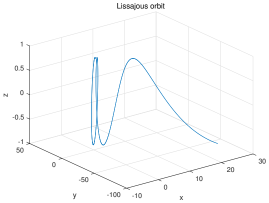

Lissajous orbit and unstable manifold

$A_u = 0.03,\ A_s = 0,\ A_x = 0.771,\ A_z = 0.906$

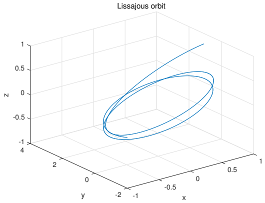

Lissajous orbit and stable manifold

$A_u = 0,\ A_s = 0.655,\ A_x = 0.771,\ A_z = 0.906$

Accuracy of the linear approximation

- Given a certain state $(x, y, z, \dot{x}, \dot{y}, \dot{z})$ one can compute:
  - the acceration $(\ddot{x}, \ddot{y}, \ddot{z})$ corresponding to the full equations of motion,
  - the acceration corresponding to the linear equations of motion $(\ddot{x}_L, \ddot{y}_L, \ddot{z}_L)$
  - the residual acceleration $RA = ((\ddot{x} - \ddot{x}_L)^2 + (\ddot{y} - \ddot{y}_L)^2 + (\ddot{z} - \ddot{z}_L)^2)^{1/2}$

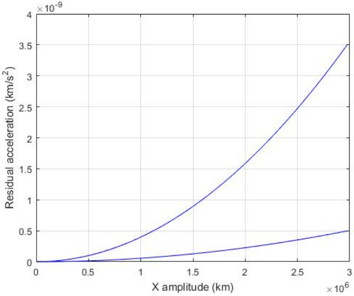

- The figure displays the maximum and average residual accelerations along "square" Lissajous orbits with $A_x = A_z \in (0.5 \cdot 10^7\, km, 3 \cdot 10^7\, km)$
- When $A_x = A_z \leq 5 \cdot 10^5 km$, then $RA_{max} \approx 10^{-10} km/s^2$

Transfers using SRP maneuvers. The basic idea

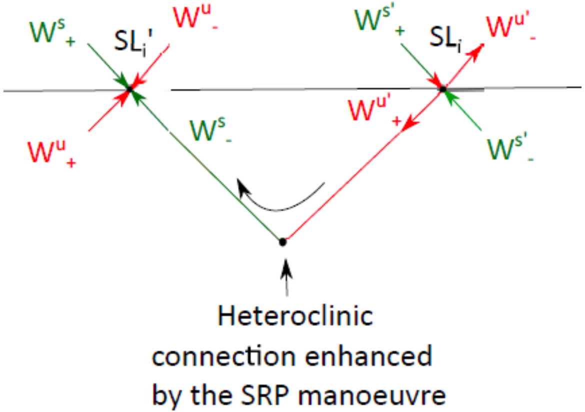

We want to perform transfers, not between equilibrium points but, between Lissajous orbits

Transfers using SRP maneuvers. Strategy

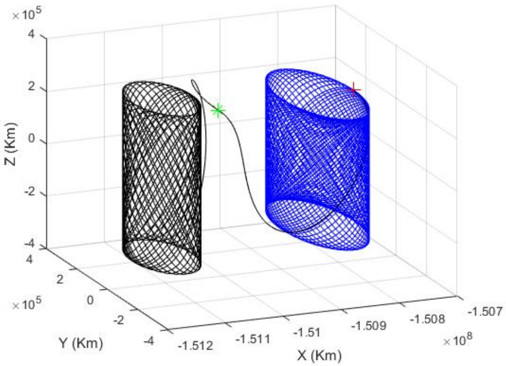

- Depart at a certain point + from a Lissajous orbit (blue) following an orbit of its unstable manifold
- At a certain point $*$ along the orbit the unstable component of the target Lissajous orbit is zero. At this point **change a sail angular parameter** that performs the transfer maneuver to an arrival Lissajous orbit (black)
- The stable component of the arrival Lissajous orbit provides convergence towards it

Transfers using SRP maneuvers. The main steps

For a fixed mass ration and once L_1 or L_2 has been selected, then:

1. Fix the departing equilibrium point (SL_i):

   Set the values of the sail parameters α, δ, and β

2. Fix the departing libration point orbit (LPO) and initial condition:

   Set the values of the in-plane and out-off-plane amplitudes A_x and A_z, the phases ϕ_1 and ϕ_2, and t_0

3. Depart along an orbit of the unstable manifold of the LPO:

   Set the stable amplitude $A_s = 0$, and unstable amplitude $A_u \neq 0$

4. At each $t > t_0$ change one or several sail parameters (SL_i will change to SL_i') and check if the unstable component, A_u', of the new LPO is zero.

5. If at some point along the departing orbit of the unstable manifold $A_u' = 0$, then perform a SRP maneuver that will insert the sail in the stable manifold of another LPO:

   If the $A_u' = 0$ condition is fulfilled, the orbit will go to the new LPO without any additional maneuver

The equilibrium point and the departing orbit and point

1. Fix the departing equilibrium point (SL_i):

   Sun–Earth mass ratio $\mu = 0.000003040$, equilibrium point L_2,
   $\alpha_i = 0$, $\delta = \pi/2$, and $\beta = 0.02$
2. Fix the departing libration point orbit (LPO) and initial condition:

   $A_x = 1/24$, $A_z = 1/6$,
   $\phi_1 = 0$, $\phi_2 = 0$, $t_0 = 0$
3. Depart along an orbit of the unstable manifold of the LPO:

   $A_s = 0$, $A_u = 10^{-4}$

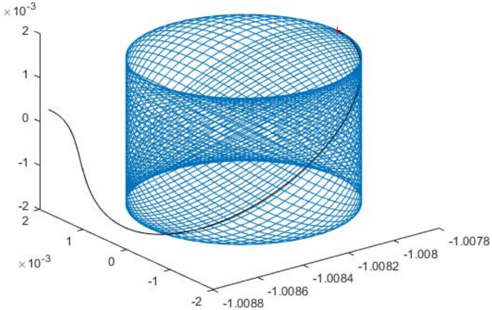

Behaviour of A'_u as a function of the transfer time

4. At each $t > t_0$ change one or several sail parameters (SL_i will change to SL'_i) and check if the unstable component, A'_u, of the new LPO is zero.

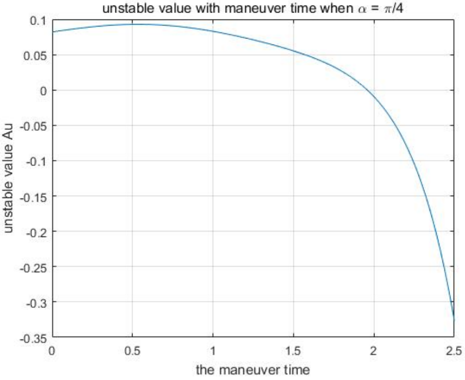

- Evolution of the final unstable amplitude A'_u when α changes from $\alpha_i = 0$ to $\alpha_f = \pi/4$
- $A'_u = 0$ for $t \approx 1.9$ (maneuver time)

The SRP maneuver

5. If at some point along the departing orbit of the unstable manifold $A'_u = 0$, then perform a SRP maneuver that will insert the sail in the stable manifold of another LPO:

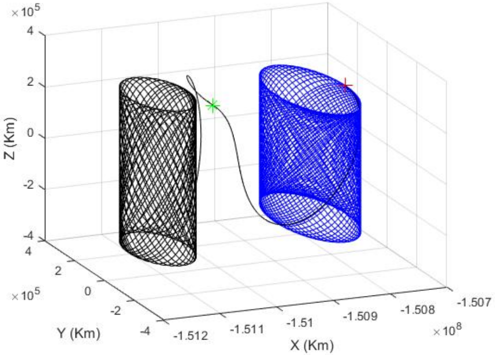

- At $t \approx 1.9$ ($A'_u = 0$) the SRP maneuver is performed changing α from $\alpha_i = 0$ to $\alpha_f = \pi/4$
- The red cross indicates the departing point along the unstable manifold of the initial orbit, the green cross is the maneuver point

Different values of α_f provide different transfers

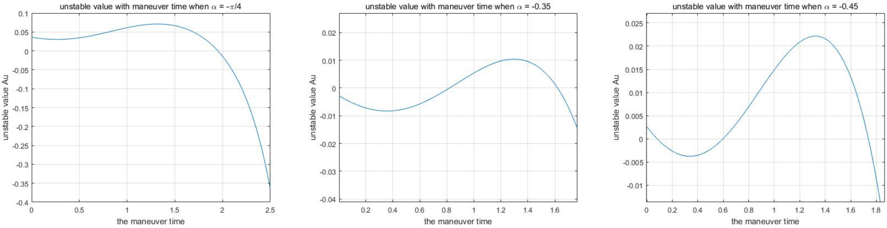

Behaviour of A_u vs time for:

- $\alpha_f = -\pi/4$ (one $A'_u = 0$ crossing)
- $\alpha_f = -0.35$ (two $A'_u = 0$ crossings)
- $\alpha_f = -0.45$ (three $A'_u = 0$ crossings)

The resulting transfers

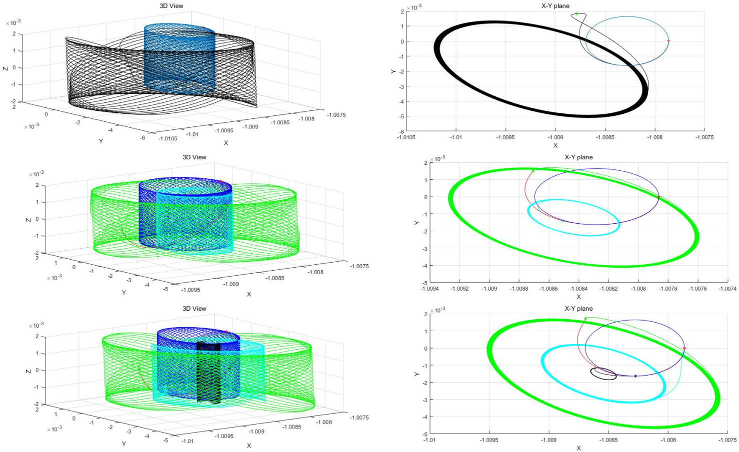

Initial and final Lissajous orbits associated to the transfers determined for $\alpha_f = -\pi/4$ (one $A'_u = 0$ crossing), $\alpha_f = -0.35$ (two $A'_u = 0$ crossings), and $\alpha_f = -0.45$ (three $A'_u = 0$ crossings)

The resulting transfers for $\alpha_f < 0$

1. When $\alpha_f \in (-\pi/2, -0.52)$ there is only 1 crossing with $A'_u = 0$
2. When α_f varies between –0.52 and –0.50, the number of crossings with $A'_u = 0$ goes from 1 to 3

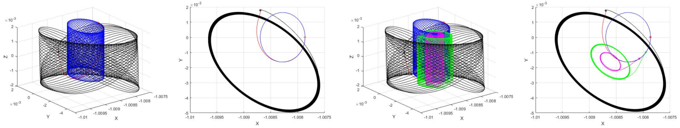

3. When $\alpha_f \in (-0.50, -0.42)$ the number of crossings with $A'_u = 0$ is 3
4. When α varies between –0.42 and –0.40, the number of crossings with $A'_u = 0$ goes from 3 to 2

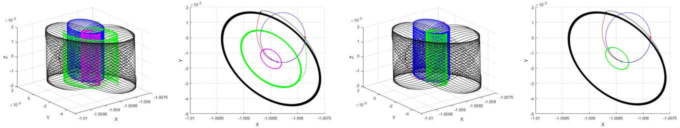

5. When $\alpha_f \in (-0.40, -0.23)$ the number of crossings with $A'_u = 0$ is 2
6. When α varies between –0.23 and –0.20, the number of transfers goes from 2 to 0, and for $\alpha_f \in (-0.20, 0.0)$ there are no crossings

Planar and vertical amplitudes of the final Lissajous orbits, and maneuver time, for cone angle maneuvers with $\alpha_i = 0$, $\alpha_f \in (-\pi/2, \pi/2)$

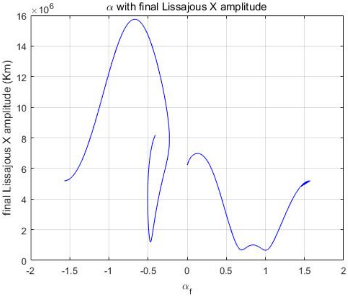

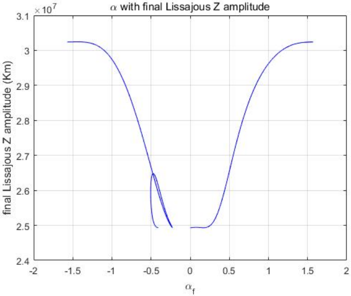

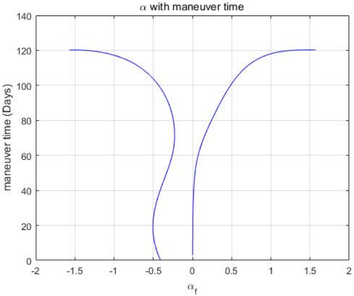

Evolution of the planar A_x and vertical A_z amplitudes of the final Lissajous orbits for cone angle maneuvers with $\alpha_i, \alpha_f \in (\pi/2, \pi/2)$

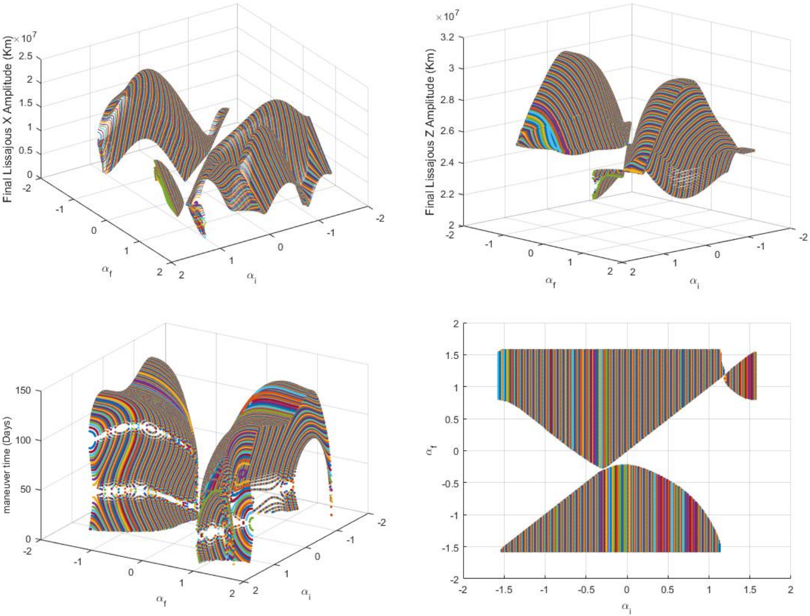

Exploring the transfer possibilities of all the orbits of the unstable manifold

- In the preceeding results only one orbit of the unstable manifold of the departing Lissajous orbit was used: $\phi_1 = \phi_2 = 0$
- For the same departing Lissajous orbit ($A_x = 1/24$, $A_z = 1/6$), and keeping $\delta_i = \delta_f = \pi/2$, we have explored the transfer possibilities using all the orbits of the unstable manifold: $\phi_1, \phi_2 \in (-\pi/2, 3\pi/2)$

Exploring the transfer possibilities of all the orbits of the unstable manifold

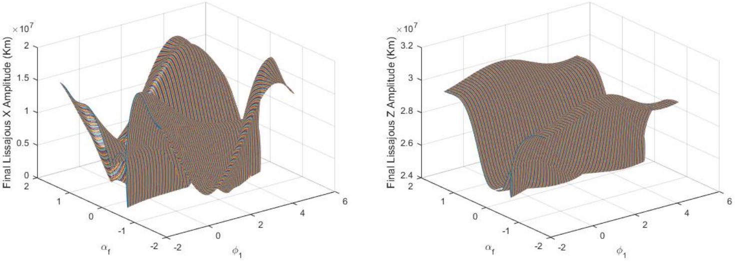

$\phi_1 \in (-\pi/2,\ 3\pi/2)$

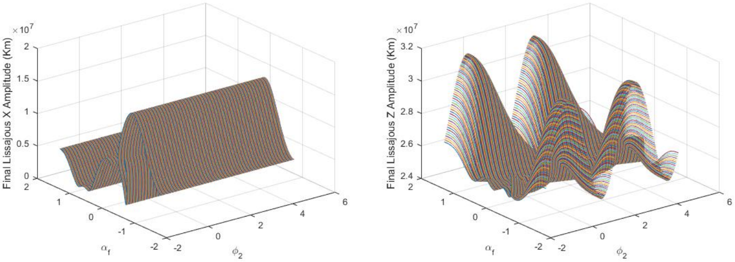

$\phi_2 \in (-\pi/2,\ 3\pi/2)$

Other kind of maneuvers. Changing δ and β

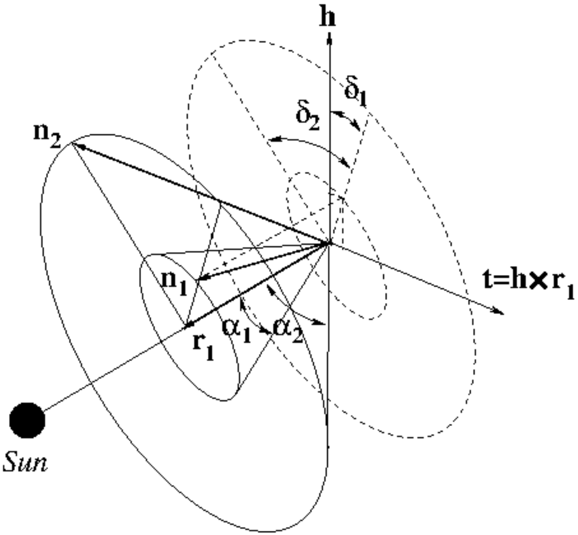

Exploring the transfer possibilities changing the clock angle δ

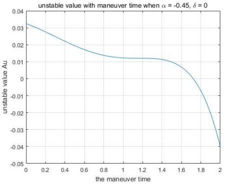

$\delta_i = \pi/2$, $\delta_f = 0$ (one $A_u = 0$ crossing)

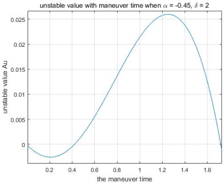

$\delta_i = \pi/2$, $\delta_f = 2$ (two $A_u = 0$ crossings)

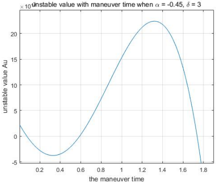

$\delta_i = \pi/2$, $\delta_f = 1.6$ (three $A_u = 0$ crossings)

- When the transfer maneuver is $\Delta\delta = \delta_f - \delta_i$, there are three different situations, according to the number of crossings with the $A_u = 0$ axisof the curves $A_u(t)$, associated to different δ_f values.
- The parameters of the simmulations are: $A_u = 10^{-4}$, $A_s = 0$, $A_x = 1/24$, $A_z = 1/6$, $\phi_1 = \phi_2 = 0$, $\alpha_i = 0, \alpha_f = -0.45$

Exploring the transfer possibilities changing the clock angle δ

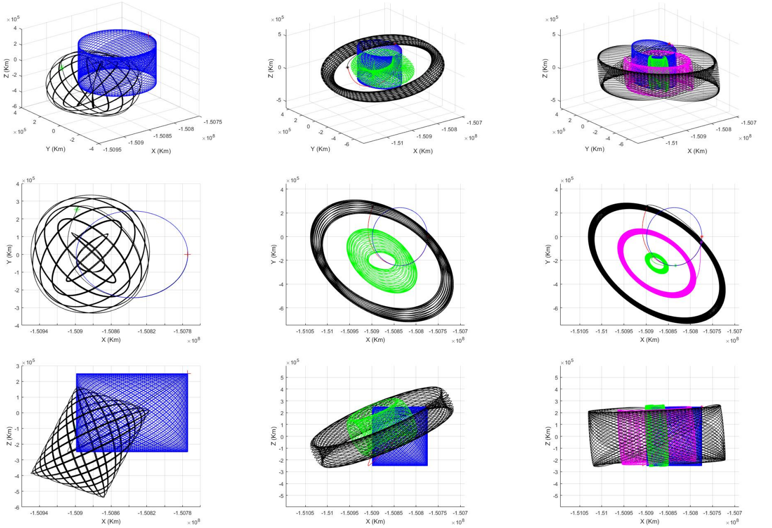

$\delta_f = 0$ (one $A_u = 0$ crossing) | $\delta_f = 2$ (two $A_u = 0$ crossings) | $\delta_f = 1.6$ (three $A_u = 0$ crossings)

Thank you very much for your attention

Other kind of maneuvers. Back and forth maneuvers

We can consider the possibility of changing the coefficient of reflectivity β by switching its value from 0.0 to 0.01 and vice-versa

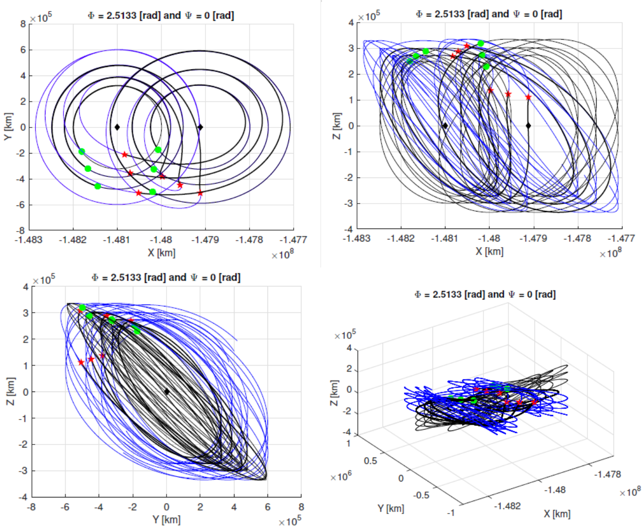

Other kind of maneuvers. Back and forth maneuvers

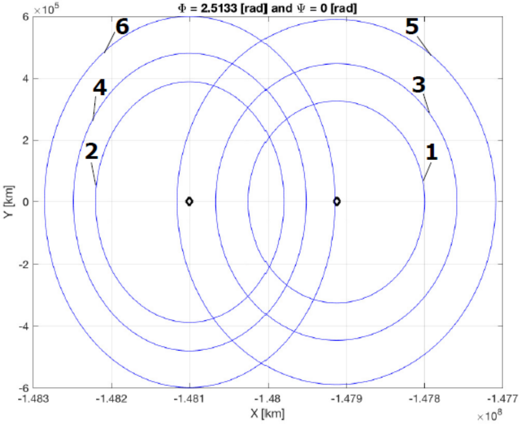

XY projection of the Lissajous involved in the back and forth β switch. The orbit labelled with number 1 is the starting orbit. The the back and forth β switch is performed between the orbits: 1-2 (forth), 2-3 (back), 3-4 (forth), 4-5 (back) and 5-6 (forth)